2011 American Control Conference
on O'Farrell Street, San Francisco, CA, USA
June 29 - July 01, 2011

Design of a Robust Vision-Based Sensor of Position and Rate for the Guidance of Autonomous Underwater Vehicles

Mario A. Jordán, Carlos Berger and Jorge L. Bustamante

Abstract— **This paper is concerned with the design of a vision-based algorithm for on-line estimation of position and rate control errors in the guidance of autonomous underwater vehicles for path tracking of underwater lines. The algorithm uses techniques of pattern recognition with different degrees of morphological operations. *Ad-hoc* experiments with a subaquatic vehicle in a test tank show the features of our approach under strong conditions of light perturbations and cloudy water.**

I. Introduction

The world of subaquatic vehicles is being expanded continuously. Applications embrace not only the classical ones of the off-shore industry but also have begun to get widely into oceanographic and scientific applications [1].

This paper deals with one of the most relevant technical application concerning path tracking of lines over the sea bottom [2]-[3]. In the general case control actions are constructed by sonar signals from the navigation system (usually provided by a side scan sonar or a multibeamer). Rarely it is fallen back on systems that are based on image motion (egomotion) provided, for instance, from an onboard camera in the vehicle. One reason may be the poor state of the water, which may be cloudy and muddy [4]. Therefore, the design of vision-based guidance systems with blurred vision come into consideration in scenarios when the altitude to bottom is relatively small. This in turn restricts the applications to a particular class of vehicles that possesses the ability to react rapidly in order to bypass potential obstacles on the sea floor.

However achieving real-time processing of blurred frames is not a trivial goal because of the diverse and numerous operations involved. They may range from a simple image conversion to gray scale up to complex pattern-recognition techniques.

In any described scenario above, an intelligent vision sensor to extract motion properties from images on the sea floor could be significant for autonomous navigation and in any case could be a complement of other navigation sensors [5]-[6].

Image-based sensors have the ability to provide information of position and velocity through image processing with certain index of confidence. A combination of techniques like pattern recognition and optical flow is a common way to build up this kind of sensors [7]-[8].

Corresponding Author: Mario A. Jordán: E-mail: mjordan@criba.edu.ar. Address: CCT-CONICET. Florida 8000, B8000FWB, Bahía Blanca, ARGENTINA

Mario Jordán, Carlos Berger and Jorge Bustamante are with the Argentine Institute of Oceanography (IADO-CONICET) and Dto. de Ingeniería Eléctrica y de Computadoras (DIEC-UNS), Bahía Blanca, Argentina.

One of the problems in the design of visual robust sensors is commonly the growth of uncertainty in the estimations under extreme situations in subaquatic environments. For instance, the usually changes of light intensity which make very difficult the information retrieval from image motion . Also blurred scenes despite adequate lighting are common in fluid medium so that the object recognition can not easily be achieved with continuity like in the aerial medium. Finally exogenous perturbations, like caustic waves on the sea floor are quite hard to filter in the context of optical flow.

One indispensable step in the design is the evaluation of sensors to be able for control purposes [9]. This step could be advantageously done in the context of teleoperation before designing an autonomous controller. So, the presence of eventual "holes" in the provided sensor information can be better anticipated in a previous study supported by teleoperation. As result, robust properties can be conferred to the sensor in order for the future control loop to be reliable.

In this paper, the design of a vision-based sensor for spacial and kinematics measurements simultaneously is focused. So we develop independently two algorithms to this end and then we concatenate them interactively for navigation in the context of path tracking of lines. A previous study for enhancing sensor robustness is pursued by means ad hoc experiments via teleoperation.

II. Vehicle Dynamics

The dynamics of the underwater vehicle is generally described by (*cf* [10])

$$\begin{aligned} M\dot{\mathbf{v}} &= -C(\mathbf{v})\mathbf{v} - D(|\mathbf{v}|)\mathbf{v} + \mathbf{g}(\boldsymbol{\eta}) + \boldsymbol{\tau}_t \\ \dot{\boldsymbol{\eta}} &= J(\boldsymbol{\eta})(\mathbf{v} + \mathbf{v}_c), \end{aligned}$$

with $\boldsymbol{\eta}$ being defined as the generalized position in some earth-fixed frame, $\mathbf{v}$ the generalized velocity vector in a vehicle-fixed frame, $\mathbf{v}_c$ is the current flow rate in vector form. Also there are system matrices, namely: the inertia matrix M, the Coriolis matrix C and drag matrix D. Besides, $\mathbf{g}$ is the net buoyancy force and $\boldsymbol{\tau}_t$ the generalized force of the thrusters. Finally, J is the well-known rotation matrix.

For autonomous vehicles, the achievement of a stationary horizontal position is important to accomplish a stable image of the ground without undesired effects of rotations due to roll and pitch. Bearing in mind a vision-based path tracking, we will refer them to as significant and less important modes. The significant ones contain the position variables in η namely x and y, but also the rotation variable ψ (yaw angle). The remainder variables in η, namely the roll θ and pitch ϕ angles are supposed inherently damped or automatically

regulated independently of the path tracking goal. Finally, the altitude z is also assumed to be regulated by autopilot to a fixed value.

III. Vision-based sensor

In the framework of tracking a line, actually only the local relative position of the vehicle with respect to the line is required. In this sense, the sensed local position provides the geometric error for a given path-tracking controller. This includes the location of the vehicle over the line and its tangential orientation. Moreover, the quantification of the motion is necessary to push the vehicle at desired cruise velocities.

In our goal, the identification of geometric and kinematic variables of the vehicle is accomplished by vision with the help of an onboard camera. This will provide the relative position x, y, the course ψ, the cruise velocity v and the rotation rate $\dot{\psi}$. All these estimations must be provided by the image moving (the so-called egomotion).

In order to abstract geometric and kinematic properties from the relative motion, some texture characteristics of the line and/or of the floor are indispensable. To this end, we have focused the sensor design in this work to fit the characteristics of a patterned line like the one depicted in Fig. 1 (see also Fig. 3).

IV. Geometric feature abstraction

Once the line is visualized in the frame, the position parameters are the slant α and the coordinates of the midpoint of the line stretch with respect to the frame center (see Fig. 1). Both α and the position coordinates are related to ψ and x, y, respectively.

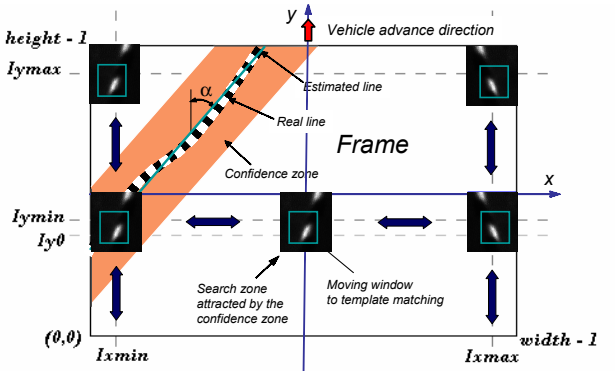

Fig. 1 - Pattern matching procedure when the estimated line moves crossing completely the frame or partially sidelong (this case is illustrated here)

The core of the sensor functions is the vision-based recognition of the line stretch. Upon this, the position parameters are determined.

In the following we develop an estimation algorithm to perform these ends. We depart from a flow of frames that arrive the estimator. Every cycle is composed by a number of operations and transforms carried out on the frame. The mathematical description of the cycle steps are given in details in [12]. We only enumerate the step functions:

A) Image conversion to gray scale

Usually, a RGB-format image is received and transformed into a grey scale.

B) Thresholding

In order to distinguish objects by contrast a binarization process is started. Commonly the pattern appear as non connected white regions (white speckles). For our purposes, detectable speckles which are part of the patterned line are as a rule totally white (without black interior).

C) Noise filtering

The differentiation between exogenous speckles and the sought-after ones in a binary image can be done by a morphological filtering. After two successive erosions, a dilation operation is carried out in order to recuperate the size of the original speckles that are not erased. Small speckles are generally produced by caustic waves on the floor in shallow water.

D) Contour detection

The resulting binary image can be further simplified. So the next goal is to work with contours only. They preserve the whole information we are needing for next identification tasks. The best method to this end is based on the morphology of the speckles. Contours can be obtained by substracting the dilation and the erosion of the binary image. Particularly, is adequate describe the contours as sequences as they are sparse in the number of pixels. In this way the levels of processing can be maintained relatively low. In case of an empty one picks up the next frame in step K).

E) Counting of detected objects

At this stage small contours (little regions that pass the previous erosions) are eliminated . One counts finally the number of contours. If there are not sufficient contours or not at all, one picks up the next frame in step K).

F) Centroids determination

A further reduction of information is attained by replacing the contours by their centroids.

G) Selection of centroids within the confidence zone

From all calculated centroids there are only those taken into account that are in the so-called confidence zone. This zone is a band delimited by two parallel lines. The outtake of centroids is performed by an ad-hoc flag.

H) On-line estimation of line stretch

If there is no, at least one, pair of flags with the logical value TRUE, one picks up the next frame in step K).

On the contrary, one searches for a line that better fits in the sense of least squares the alignment of the centroids in the confidence zone. So the slope of the estimated line (referred to as α) and the midpoint of the visible segment of the line determine the parameters of the estimated line.

I) Statistic correction

With the sake of reducing the number of wrong estimations and giving certain continuity to the algorithm in the identification of the line, some statistical modifications are introduced. Also the contribution of this step would be to make the algorithm more robust against perturbations. The modification takes into account results from previous cycles. Two algorithm were comparatively tested.

a) Method of the affine data averaging.

One defines an affine parameter $\lambda$with $0 \leq \lambda \leq 1$ that weighs present and past data in the estimation. It can be also adapted in the commissioning phase and change conveniently later in the context of a supervision program.

b) Method of the forgetting factor

Here λ has the same range as before, but the discard of past data is not abrupt but exponential. So the influence of past data vanish as the cycles goes on. Here the employment of a forgetting factor λ has proved to be very effective although also we have compared the results with averaging of past data.

J) Adaptation of the confidence zone

It is important to adapt permanently the confidence zone, because the conditions of the image are commonly changeable. One possibility is to adjust the width in the proportion of the speckle areas, or alternatively, the simple count of the pixels conforming any contour gives idea of the order of magnitude of the change of the width. Another possibility could be to let the border lines of the confidence zone be not parallel.

K) Take the next frame

Return to step A).

V. KINEMATICS FEATURE ABSTRACTION

The second function of the sensor concerns the kinematic estimation from egomotion. Generally spoken, the previous algorithm to estimate relative position of the line is taken as basis to work up to a new combined procedure. Once again, we will emphasize the requirements of real-time calculations so as to estimate measures on line for a future guidance control system. This goal is hard to achieve when parameters have to be extracted from image processing on-line.

We here developed a kinematic algorithm which takes full advantage of the previous geometric algorithm. The readers are referred to [11] and [12] for more details.

The novelty in this work is the combination of the geometry and the kinematics estimation in a complete sensor.

The key idea in this module is to define a search zone over the patterned line and the overlapping the confidence zone as close as possible (see Fig. 1). Inside it, there is a small moving window in where the pattern matching of a template will take place. This window slides slightly everywhere in all directions to pattern matching, but always enclosed in the search zone.

Clearly, the recognition of motion properties is related to techniques of optical flow. Since in general common optical flow techniques are markedly time-consuming and considered not fit for control systems with rapid response, we will develop a simple but robust correlation-based method instead.

First, we describe features of the problematic in order to afterwards be able to organize the estimation steps.

A. Attracted search zone

One of the problems to be tackled in our goal is to share the search zone in the confidence zone when, for instance, the line is moving fast in the vision frame. This can occur, above all, when perturbations affect the control system and control actions do not avoid that the line slides rudely from the frame center. Obviously, this problem is quite alien to the vision-based sensor. However it is aimed by design to confer robust properties to search procedure, that makes the sensor more reliable. To this goal the search zone is continuously being attracted by the confidence zone. In that way, if the line is visible in the frame through the confidence zone, a pattern matching is possible.

B. Time scale correction

In order to avoid wrong velocity estimation due to perspective projection, and since the equations that relate the intrinsic camera parameters with the parameters involved in the projection of 3D scenes onto the image plane are strongly non-linear (radial-and tangential-distortion effects), we have aimed a much more simple solution to time scale counterbalance. This consists in searching the patterns horizontally at a constant height in the frame (see Fig. 1). This is carried out basically when the line crosses completely the frame and cuts the top and bottom borders of the frame. The criterion to select the constant height to slide the search zone is oriented twice, first to a good local vision quality in the frame (it is, with an appropriate sharpness), and second to the stability of the pattern matching.

In cloudy and blurred waters, the best image quality occurs approximately just about the lower border of the frame (minimal distance between camera and target), however by large outgoing pattern velocities there exists the risk of losing them and consequently causing the interruption of the algorithm. For those reasons, the optimal region is defined just beneath the horizontal middle line. It can also occur that the line moves sidelong and cuts the left or right borders of the frame. So, in this case we let the search zone to glide vertically up and down following the center of the confidence zone.

C. Pattern matching

Let us suppose the search region stays overlapping the confidence zone and a template with a pattern was selected in the moving window a sampling time before. This template has specific coordinates (x_{t-1}, y_{t-1}). After Δt seconds a new frame enter the algorithm to be processed at the present sampling time. So, the search zone slides eventually a bit so as to overlap the new position of the confidence zone. Then the moving window inside the search zone begins the matching process by correlation between the previous template and the window contents. Varying the template coordinates for the moving window in all directions, a maximum of the correlation is searched for. This maximum occurs by successful matching, say at coordinates (x_t, y_t). From this value on, an actual value of the velocity is estimated as the incremental quotient $\hat{v}_t = \frac{(x_t,y_t)-(x_{t-1},y_{t-1})}{\Delta t}$.

It is worth noticing that the estimation suffers from quantification errors and false perspective appreciation which are proper from 2D image approaches. In fact, effects of radial and tangential distortions are not taken into account. So the evolution of the estimates may be irregular and a filtering is needed. This is accomplished in two ways. On one

side, a filter of maximum difference is used to reduce high fluctuations that appears in some cases concerning images with elevated noise level (change of contrast, caustic waves, etc.). On the other side, a strong perturbation may be induced when the estimated position of the line is incorrect. In such a cases, the calculated value $\hat{v}_t$ is averaged with the previous value $\hat{v}_{t-1}$.

Moreover, this filtering is not sufficient enough to smooth the time evolution of $\hat{v}_t$ according to the expected quality for control purposes. Therefore a second filter with a forgetting factor allows a much more soft time evolution.

It is to remark that the estimations are displacements expressed in pixels, so the velocity is measured in units of pixels/frame. Knowing the frames per second of the camera , one can obtain velocity in units of pixels/second.

Finally, a commissioning face will allow us to determine parameters to tune the algorithm in order to give the vehicle velocity in the physical units meters per second. Among these parameters are the altitude, the tilt angle of the camera, the extrinsic and intrinsic parameters of the camera, and proper parameters of the image processing. Moreover, it is supposed that an autonomous vehicle possesses an autopilot to regulate altitude as well as to select a proper camera tilt angle according to a convenient shortsighted or large-sight vision of the bottom scene. Due to space limitations in the paper we will not address the calibration procedures here.

D. Algorithm to rate estimation

A) Initialization at first frame

The template is located at the confidence zone according to possible displacement regions. The search zone is defined for the next frame around template location.

B) Acquisition of a new frame

C) Estimation of line position and angle

Use algorithm for spatial feature abstraction

D) Pattern matching

Here a match based in correlation of the previous template with contents in the moving window inside the search zone is performed.

E) Kinematic feature estimation

Determination of the template displacement as the sliding point that produces the maximum correlation value.

F) Apply "maximum difference" filter

G) Apply "statistic correction" filter"

H) Select new template

Calculation of coordinates of the search zone . Adjustment of template initial position.

I) Return to step B)

VI. Supervision algorithm

It is quite important for successful vision-based control applications that the sensor can give the controller a certain confidence about the quality of measures.

In customary operations, pattern estimations may fail: *a*) due to bad sporadic image quality or *b*) simply when patterns actually ran over the frame. In order to identify such conditions, supervision is needed. This should provide a flag, to stop estimations of position and rate in the two abnormal conditions, and also to continue estimating when such conditions have disappeared (case *a*) or have been remedied by control (case *b*).

A. Presence and quality detector

To this end, a new module that performs histogram-based operations is included in the whole algorithm. It works upon the observed fact that both images of patterns and of the sea floor alone, have typically distinct statistic properties when contrasted. For instance, as seen in Fig. 2, the histogram of a pattern is typical bimodal (two local maximums) and well extended over the range [0, 255] due the high contrast between black and white zones. On the other hand, the environment on the bottom has a narrow range of intensities instead (one typical maximum) with poor contrast. This last scenario can also appear by blurred image even when the pattern is in focal plane.

Accordingly these differences will be exploited here for detecting "pattern presence/absence" or "bad/good measure quality"

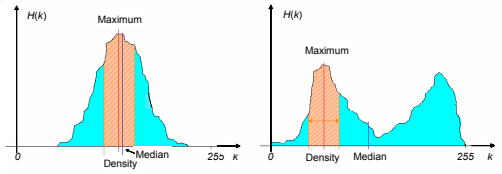

Fig. 2 - Left: histogram of sea floor. Right: histogram of pattern

B. Algorithm for image classification

1) Calculate the histograms on ROI´s (Region of Interest) around the estimated pattern
2) Find maximum value of histogram
3) Calculate density ρ around this maximum
4) Find median
5) Calculate standard deviation σ
6) If $(\sigma > \sigma_{min})$ and $(\rho < \rho_{max})$, one concludes the pattern is visible in the ROI, otherwise the ROI only contains image of the sea floor (sensor failure).

Parameters σ_{min} and ρ_{max} are adjusted according to the underwater image quality. Typical experimental values were found about 95% and 30 units, respectively.

Selected ROI´s are commonly set on the image corners and center. Once the pattern is located again after a sensor failure, estimation modules are reset and sensor continues working in normal estimation mode.

VII. Experiments

A. Setups

To test the vision-based approach, a series of experiments in a test tank were set up. These consisted in the employment of a subaquatic vehicle (AUV prototype, see Fig. 4) that navigates by telecontrol, following a visible path on the tank bottom. The vehicle possesses a wireless camera onboard that transmits the images during the egomotion. For the path tracking purposes a patterned line which is bent according to any circuital form is employed (see Fig. 4). In many performed experiments there were perturbations of wind producing currents from some slanted direction, or of caustic

waves on the floor produced by the sun rays at midday when trespassing an undulating free surface.

One fact to be highlighted is the altitude of the vehicle with respect to the bottom. Motived by the different states of water transparency, we have mounted the vehicle motion at two different constant altitudes. In the time the experiments were realized the water transparency was changing from very transparent to cloudy during the weeks. The results shown in the paper, pertain to the first and the last phase. These in turn have forced us to set the experiments up in a shortsighted and longsighted vision-based navigation.

In order to evaluate the sensor performance for control purposes in a closest-real environment, we took advantage of the teleoperation which provided the image motion with the line visualized inside the frames.

B. Position and rate identification

Several experiments were led with the described setups. We will illustrate one of them in Fig. 5. Here some cycles are selected to show the features of the sensor algorithm in normal and critical situations. From the left and to the right of the figure, we can see photograms of the line in a shortsighted and longsighted orientation of the camera.

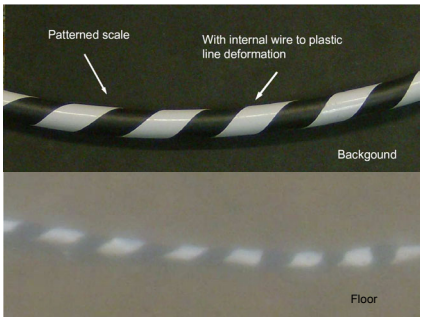

Fig. 3 - Experimental line for path tracking. Top: line in air. Bottom: line in water

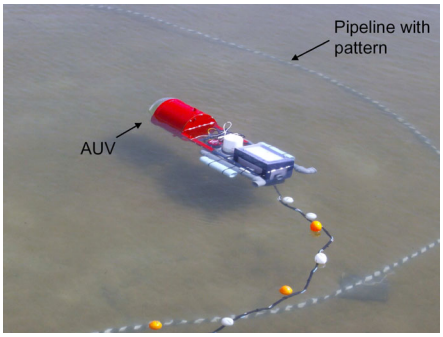

Fig. 4 - Navigation in open-air tank with reference line

The on-line estimation of the line is drawn in the image together with its confidence zone according to the algorithm described before. The rate of frames processing was about 10 frames per second which gives small sampling times for control purposes at large cruise velocities in subaquatic vehicles. However, when combining the position and the kinematic jointly, the measurement rate is reduced in half the time.

We now describe in more details the Fig. 5, left, corresponding to the navigation with shortsighted horizon. In a) the position estimation gave a false line position, and consequently the velocity value was incorrect in this frame. In b), the rapid movement of vehicle produces a lost of the line in the respective frame, thus also here nor a rate estimation neither the line location was possible. Once a line is well detected, the velocity estimation can be realized error free. This occurred in c) where a good image arrived and a successful estimation was resulted. In d), the estimation is also correct although image quality decreases. A vertical displacement restriction had occurred in e) when the line moved sidelong to the right border of the frame. This executed the pattern-matching process on the borders. In f)-g) two scenarios are shown related to when the templates came back in the center of the image and the search zone had begun to slide horizontally for pattern matching.

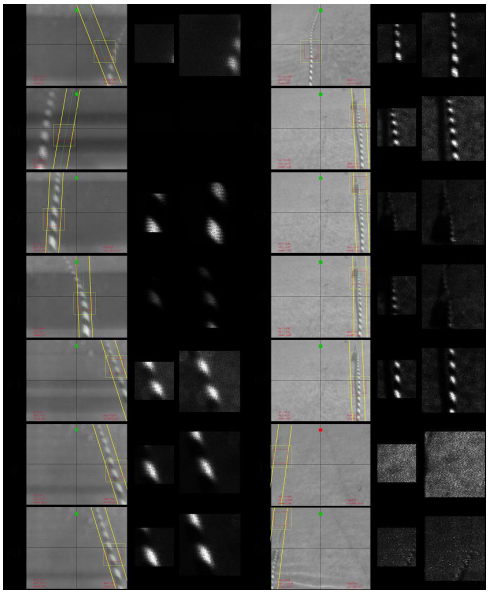

Fig. 5 - Selected frames for navigation with shortsighted and longsighted horizons

Similar results are shown in Fig. 5, right, for the navigation with longsighted horizon. In a) the scenario when the position estimation did not give the right line location is illustrated, but the velocity estimation could be realized anyway. In b), the search zone was attracted by the confidence zone which crossed vertically the frame causing the moving window to search for pattern over the horizontal middle line. In c), the limit case is shown when the confidence zone was moving to the right up to touch the lateral border. Up to here the line began to cut the lateral right border and from this time on the pattern matching was consequently be accomplished sidelong. This allowed continuity in the rate estimation. This last process ended when the control forced the confidence zone to enter again in the frame interior in direction to the left, see d)-e). Here the search zone came down and slid over the middle horizontal again. In f) the pattern went out of image because of the poor quality of the frame, so the estimated values became spurious until the pattern could be detected in g). The navigation with camera in the longsighted orientation seems to provide a wide vision field and so the line may

be much better detected than in the case of shortsighted horizon. Also the control could allow itself to compensate large path errors due to strong perturbations. However this scenario can change drastically by blurred waters in where the altitude has to be diminished and the camera horizon has to be tuned to a rather shortsighted vision as occurred in our experimental case studies.

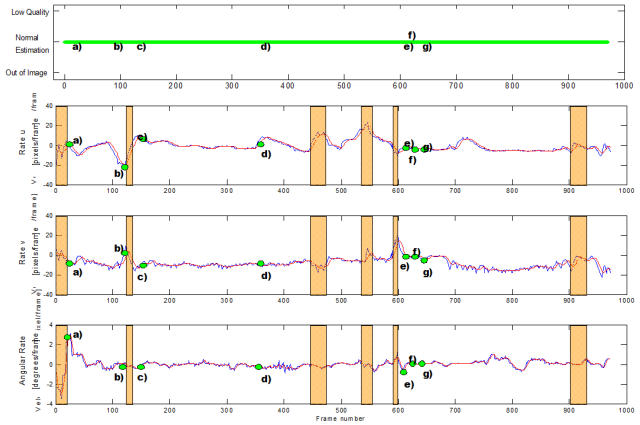

Fig. 6 - Estimation of the advance velocity from the vision-based sensor in a shortsighted-horizon setup

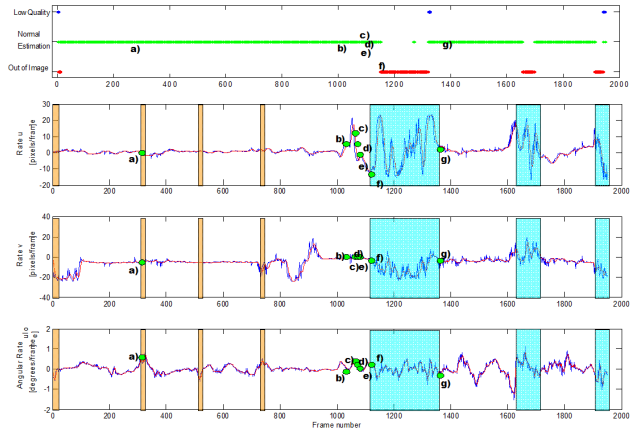

Fig. 7 - Estimation of the advance velocity from the vision-based sensor in a longsighted horizon setup

In Figs. 6 and 7 we will illustrate the evolution of the final conditioned estimated rate in their components and in the two cases related to shortsighted horizon (Fig. 6) and longsighted horizon (Fig. 7). Moreover, for the sake of clarity, there were indicated with marks the cases a) up to g) for which the frames were shown in Fig. 5. Also windows (in orange) showing the periods when the pattern matching was accomplished on the lateral borders were indicated in both figures. Similar indication in windows (in blue) was carried out for the cases when the line got lost or could not being identified from reasons of poor quality of the image. These windows were located manually after seeing the processing, and they helped us to analyze the flag evolution given by the supervision algorithm.

Clearly, it can be seen that the continuity of the rate estimation is maintained in the transitions when the search zone moves horizontally and then slides vertically sidelong and vice versa. However, when the line could not be located, the estimation showed signs of instability, turning oscillatory and irregular. This had occurred only in the longsighted orientation of the camera. In this case, the flag indicating estimation quality performs adequately almost all the time. Incorrect matching cases from the main algorithm can not be discriminate with the proposed supervision.

VIII. Conclusions

This paper was concerned with the design of a vision-based algorithm for on-line estimation of position and rate during path tracking of patterned lines. The algorithm employes techniques of pattern recognition with different degrees of morphological operations and pattern matching upon image correlation. The developed techniques had shown to be able to ensure continuity of the estimation even in blurred waters. When sporadic failures causing lack of continuity occur, an ad hoc supervision algorithm generates alarms which would be necessary in a control context. Additionally, it was established that the proper tuning of the camera horizon is significant for the success of the estimations. Ad hoc experiments with a subaquatic vehicle in a test tank had shown the feasibility of our approach under strong conditions of light perturbations and cloudy water. A vehicle teleoperation for tracking of a patterned line on the floor, provided the flow of frames in a closest-real environment for the evaluation of the sensor performance.

References

[1] M. Narimani, S. Nazem and M. Loueipour, "Robotics vision-based system for an underwater pipeline and cable tracker," in *OCEANS'09*, Bremen, Germany, May 11-14, 2009. pp. 1-6

[2] A. V. Inzartev (Editor), *Underwater vehicles*, In-Tech, Vienna, 2009.

[3] Y. Wang and I.I. Hussein, "Cooperative Vision-Based Multi-Vehicle Dynamic Coverage Control for Underwater Applications," in *IEEE Int. Conf. on Control Applications (CCA 2007)*, Singapore, Oct 1-3, 2007, pp. 82 - 87.

[4] J. Sattar and G. Dudek, "On the performance of color tracking algorithms for underwater robots under varying lighting and visibility" in *IEEE Int. Conf. on Robotics and Automation (ICRA 2006)*, Orlando, USA, May 15-19 2006, pp. 3550 - 3555.

[5] J. Sattar, G. Dudek, O. Chiu, I. Rekleitis, P. Giguere, A. Mills, N. Plamondon, C. Prahacs, Y. Girdhar, M. Nahon and J.-P. Lobos, "Enabling autonomous capabilities in underwater robotics," in *IEEE/RSJ Int. Conf. on Intelligent Robots and Systems (IROS 2008)*, Nice, France, Sept. 22-26, 2008, pp. 3628-3634.

[6] A. Huster, E.W. Frew, S.M. Rock, "Relative position estimation for AUVs by fusing bearing and inertial rate sensor measurements," in *OCEANS'02,* Mississipi, Oct. 29-31, 2002, vol. 3, pp. 1863 - 1870.

[7] S.van der Zwaan, J. Santos-Victor, "Real-time vision-based station keeping for underwater robots," in *OCEANS'01*, Honolulu, USA, Nov. 5-8, 2001, vol.2, pp. 1058 - 1065.

[8] F. M. Caimi, D.M. Kocak, F. Dalgleish, J. Watson, "Underwater imaging and optics: Recent advances," in *OCEANS'08*, Quebec City, USA, Sept. 15-18, 2008, pp. 1-9.

[9] N.M. Garcia-Aracil, J.M. Azorin Poveda, J.M. Sabater Navarro, C. Perez Vidal and R. Saltaren Pazmino, "Visual Control of robots with changes of visibility in image features," *IEEE Latin America Transactions*, vol. 4 (1), 2006, pp. 27-33.

[10] T.I. Fossen, *Guidance and Control of Ocean Vehicles*, John Wiley&Sons, New York, 1994.

[11] M.A. Jordán, J.L. Bustamante, C. Berger and S. Hansen. "Two Vision-based Algorithms for Image-Properties Extraction in the Path Tracking of Underwater-Vehicle Navigation," in *XXII Congreso Argentino de Control Automático*, Buenos Aires, Argentina, Aug. 3-Sept 2, 2010.

[12] M.A. Jordán, J.L. Bustamante, C. Berger and S. Hansen. "Path Tracking in Underwater Vehicle Navigation - On-Line Evaluation of Guidance Path Errors via Vision Sensor," In *49th IEEE Conf. on Decision and Control*. Atlanta, USA, Dic.15-17.